
Continual evaluation for lifelong learning: Identifying the stability gap

Matthias De Lange

KU Leuven

matthias.delange@kuleuven.be

Gido van de Ven

KU Leuven

gidovandeven@gmail.com

Tinne Tuytelaars

KU Leuven

tinne.tuytelaars@kuleuven.be

Abstract

Introducing a time dependency on the data generating distribution has proven to be difficult for gradient-based training of neural networks, as the greedy updates result in catastrophic forgetting of previous timesteps. Continual learning aims to overcome the greedy optimization to enable continuous accumulation of knowledge over time. The data stream is typically divided into locally stationary distributions, called tasks, allowing task-based evaluation on held-out data from the training tasks. Contemporary evaluation protocols and metrics in continual learning are task-based and quantify the trade-off between stability and plasticity only at task transitions. However, our empirical evidence suggests that between task transitions significant, temporary forgetting can occur, remaining unidentified in task-based evaluation. Therefore, we propose a framework for *continual evaluation* that establishes per-iteration evaluation and define a new set of metrics that enables identifying the worst case performance of the learner over its lifetime. Performing continual evaluation, we empirically identify that replay suffers from a *stability gap*: upon learning a new task, there is a substantial but transient decrease in performance on past tasks. Further conceptual and empirical analysis suggests not only replay-based, but also regularization-based continual learning methods are prone to the stability gap.¹

1 Introduction

The fast convergence in gradient-based optimization has resulted in many successes with highly overparameterized neural networks [23, 29, 12]. In the standard training paradigm, these results are conditional on having a static data generating distribution. However, when non-stationarity is introduced by a time-varying data generating distribution, the gradient-based updates greedily overwrite the parameters of the previous solution. This results in *catastrophic forgetting* [13] and is one of the main hurdles in *continual or lifelong learning*.

Many variations of benchmarks have been proposed to identify the efficacy of continual learning methods in alleviating catastrophic forgetting. These benchmarks are typically constructed by partitioning the data stream in discrete locally-stationary distributions, called tasks. As training of a new task is completed, performance of the learned model is evaluated using held-out datasets for all observed tasks. This framework has enabled quantifying the phenomenon of catastrophic forgetting

¹Code: <https://github.com/mattdl/ContinualEvaluation>

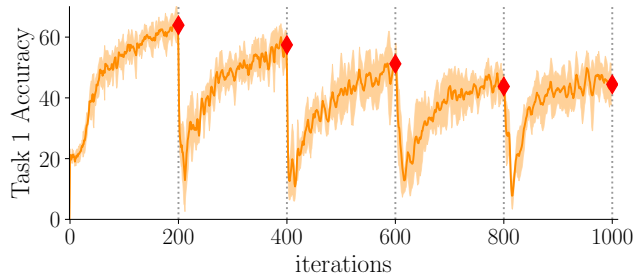
as performance drastically drops for previously observed tasks [13, 14], and has since been widely adopted [34, 25, 21, 10].

In this work, we identify limitations of this task-oriented evaluation protocol. First, our empirical evidence suggests that significant, temporary forgetting occurs *in between* task transitions, which remained unidentified so far due to the coarse evaluation periodicity on task transitions only. Second, the coarse incremental evaluation protocol is in dissent with the perspective on continual learners as agents that acquire knowledge over their lifetime, which has gained significant attention in recent literature [4, 3, 11, 6, 5]. Therefore, we advocate that continual *learning* requires continual *evaluation* to ensure the learner remains performant at all times and to establish performance analysis founded on the full learning behavior.

To this purpose, we define a framework for *continual evaluation* that evaluates the learner after each update. We establish a taxonomy of the current metrics in continual learning relevant to our study, and define a novel set of continual evaluation metrics with a focus on worst-case performance. The continual evaluation framework and metrics led us to discover the *stability gap*: a temporary but substantial forgetting of past tasks upon starting to learn something new. Figure 1 illustrates this phenomenon. Our empirical and conceptual analysis of the stability gap find shortcomings in stability of the learner for both replay-based and regularization-based methods.

We advocate that measuring continual worst-case performance is important to enable continual learners in the real world, especially for safety-critical applications and real-world actuators. Many sources of variability may affect the evolution of a data-based continual learner in unexpected ways. In this work, we highlight that even with a controlled data stream, representative continual learning methods falter in maintaining robust performance during the learning process.

Figure 1: **The *stability gap*: substantial but temporary forgetting upon learning a new task.** Shown is the accuracy on the first task, when a neural network sequentially learns the first five tasks of Mini-ImageNet using Experience Replay. Continual evaluation at every iteration (orange curve) reveals sharp, transient drops in performance when learning new tasks, i.e. the *stability gap*. This phenomenon remained unidentified with standard task-oriented evaluation (red diamonds). More details in Figure 2.



Scope. This work employs the standard supervised setup for classification in continual learning, with experiments in computer vision. We explore 4 benchmarks for our experiments in class and domain incremental learning [38]. In our detailed analysis with the continual evaluation framework, we predominantly focus our experiments on Experience Replay [16, 8, 35], as this method is known to perform consistently well over the three setups [38, 28, 10, 35], is a representative method for the family of replay-based methods [10], and has been widely adopted in literature [34, 9, 11, 7].

2 Preliminaries on Continual Learning

The continual or lifelong learning classification objective is to learn function $f_\theta : \mathcal{X} \rightarrow \mathcal{Y}$, mapping the input space \mathcal{X} to output space \mathcal{Y} with parameters θ , from a non-stationary data stream $\mathcal{S} = \{(\mathbf{x}, \mathbf{y})_0, (\mathbf{x}, \mathbf{y})_1, \dots, (\mathbf{x}, \mathbf{y})_n\}$, where data tuple $(\mathbf{x} \in \mathcal{X}, \mathbf{y} \in \mathcal{Y})_t$ is sampled from data generating distribution \mathcal{D}_t at time t . While standard machine learning assumes a static data generating distribution, continual learning introduces the dependency on time variable t . This time-dependency introduces a trade-off between adaptation to the current data generating distribution \mathcal{D}_t and retaining knowledge acquired from previous ones $\mathcal{D}_{<t}$, also referred to as the *stability-plasticity trade-off* [15].

Tasks. The data stream is often assumed to be divided in locally stationary distributions, called tasks. We introduce the discrete task identifier k to indicate the k -th task T_k with locally stationary data generating distribution \mathcal{D}_k . Additionally, we assume the time variable t is discrete, indicating the total iteration number over the stream. The last iteration t learning task T_k is denoted by $t = |T_k|$.

Learning continually. During the training phase, a *learner* continuously updates $f_{t,\theta}$ based on new tuples $(\mathbf{x}, \mathbf{y})_t$ from the data stream [11]. Optimization follows empirical risk minimization over the observed training sets $\tilde{D}_{\leq k}$, as the learner has no direct access to data generating distributions $\mathcal{D}_{\leq k}$. The negative log-likelihood objective while learning task T_k at iteration t is defined as:

$$\min_{\theta} \mathcal{L}_{t,k} = -\sum_{n=1}^k \mathbb{E}_{(\mathbf{x}, \mathbf{y})_{\leq t} \sim \tilde{D}_n} [\mathbf{y}^T \log f_{\theta,t}(\mathbf{x})] \quad (1)$$

The main challenge for continual learning is to estimate this objective having only the current task's observed training data $(\mathbf{x}, \mathbf{y})_{\leq t} \sim \tilde{D}_k$ available or a subset hereof, while limiting the overhead to sub-quadratic time and sub-linear space complexity over the number of tasks.

3 A framework for continual evaluation

This section introduces a general framework for *continual evaluation* of continual learners, introduces novel metrics, and examines relaxations regarding computational feasibility.

3.1 The Continual Evaluator

The *learner* continually updating $f_{t,\theta}$ has a counterpart, the *continual evaluator*, that tracks the performance of $f_{t,\theta}$ over time. Not only the data observed by the learner in data stream \mathcal{S} may change over time, but also the goals the model should obtain. This is reflected in a time dependency on the evaluator's data stream \mathcal{S}_E [11]. The evaluator is configured by three main factors: i) the evaluation periodicity ρ_{eval} defining the interval of evaluation for $f_{t,\theta}$; ii) the process to construct \mathcal{S}_E ; iii) the set of evaluation metrics. We define *continual evaluation* solely in terms of the periodicity.

Definition. Assuming $f_{t,\theta}$ is deterministic, continual evaluation monitors the continual learning model $f_{t,\theta}$ at each atomic change that might affect its outcome.

The desirable behavior of the model can be disentangled in performance on a set of **evaluation tasks**. Similar to the tasks in the learner's data stream \mathcal{S} , evaluation tasks indicate locally-stationary distributions. We define a set of N *evaluation tasks* $\mathcal{T}_E = \{E_0, \dots, E_N\}$, where each evaluation task E_i has a data set $\tilde{D}_{E,i}$ sampled from static data generating distribution $\mathcal{D}_{E,i}$. The set of evaluation tasks can be extended at any point in time: $\mathcal{T}_E \leftarrow \mathcal{T}_E \cup \{E_{N+1}\}$. Following literature [10, 38], we assume a new evaluation task E_k is added on each encountered training task T_k in \mathcal{S} . The evaluation data $\tilde{D}_{E,k}$ may consist of a subset of the observed task training data \tilde{D}_k , or a held-out evaluation set to test the generalization performance with $\tilde{D}_k \cap \tilde{D}_{E,k} = \emptyset$.

Four main settings have been defined in literature [38, 11] based on revealing the task identifier k to the learner or evaluator and the type of distribution shift. The task identifier is available to the learner in **task, domain and class incremental** learning, and additionally to the evaluator for task incremental learning, a strong assumption that allows isolation of the task-specific output space $\mathcal{Y}_k \subseteq \mathcal{Y}$. In class-incremental learning the dimensionality of the output space is extended as new classes are observed. Domain incremental learning retains a fixed output space, but assumes shifts in the input distributions \mathcal{X}_k . **Data incremental** learning assumes k is never revealed.

3.2 Continual Evaluation Metrics

The third factor of the evaluator is the set of evaluation metrics used to assess the performance of the learner. To date, metrics have been defined mainly assuming evaluation on task transitions ($\rho_{\text{eval}} = T_i$) and focusing on the final performance of the learner. We advocate that continual worst-case performance is important for continual learners in the real world. Therefore, we propose new metrics to quantify worst-case performance (WC-ACC, min-ACC, WF^w) and metrics that are also applicable to task-agnostic data streams (WF^w, WP^w). We focus on classification metrics, with **accuracy** (the percentage of correctly classified instances) considered the main performance metric. The accuracy of evaluation task E_k on the t -th iteration model $f_{t,\theta}$ is denoted as $\mathbf{A}(E_k, f_t)$, omitting θ for brevity.

3.2.1 Stability-based Metrics

To measure stability of the learner, we aim to quantify how well knowledge from previously observed tasks $T_{<k}$ is preserved while learning new task T_k . **Average forgetting (FORG)** [7] averages the accuracy difference for the most recent model $f_{|T_k|}$ compared to $f_{|T_i|}$ just after learning T_i with evaluation task E_i , and is defined as $\frac{1}{k-1} \sum_{i=1}^{k-1} \mathbf{A}(E_i, f_{|T_i|}) - \mathbf{A}(E_i, f_{|T_k|})$. Large forgetting indicates the phenomenon of *catastrophic forgetting*, while negative forgetting indicates knowledge transfer from new to previous tasks. This transfer is referred to as **backward transfer** [7] and has been defined as a metric that is the negative of FORG [27].

For worst-case performance it is desirable to have an absolute measure on previous task performance. We define the **average minimum accuracy (min-ACC)** at current training task T_k as the average absolute minimum accuracy over previous evaluation tasks E_i after they have been learned:

$$\text{min-ACC}_{T_k} = \frac{1}{k-1} \sum_{i=1}^{k-1} \min_n \mathbf{A}(E_i, f_n), \forall |T_{i-1}| < n \leq t \quad (2)$$

where the iteration number n ranges from after the task is learned until current iteration t . This gives a worst-case measure of how well knowledge is preserved in previously observed tasks $T_{<k}$. In the following, we report the min-ACC for the last task, omitting the dependency on T_k for brevity.

Furthermore, we introduce a more general stability metric that does not assume a task-based data stream, and is therefore also applicable to data incremental learning. We define **Windowed-Forgetting (WF^w)** based on a window of w consecutive accuracy evaluations averaged over the evaluation set \mathcal{T}_E . For a single evaluation task E_i the maximal accuracy decrease in the window $\Delta_{t,E_i}^{w,-}$ and the task-specific Windowed-Forgetting \mathbf{WF}_{t,E_i}^w are defined at current iteration t as

$$\Delta_{t,E_i}^{w,-} = \max_{m < n} (\mathbf{A}(E_i, f_m) - \mathbf{A}(E_i, f_n)), \forall m, n \in [t-w+1, t] \quad (3)$$

$$\mathbf{WF}_{t,E_i}^w = \max_n \Delta_{n,E_i}^{w,-}, \forall n \leq t \quad (4)$$

Averaging the metric over all N evaluation tasks results in a single metric $\mathbf{WF}_t^w = N^{-1} \sum_i^N \mathbf{WF}_{t,E_i}^w$. As it identifies the maximal observed performance drop in the window, it is considered a worst-case metric. Evaluators that can afford linear space complexity can consider the full history at iteration t with \mathbf{WF}^t . To account for both fast catastrophic forgetting and forgetting on a larger scale with constant memory, we instantiate \mathbf{WF}^{10} and \mathbf{WF}^{100} .

3.2.2 Plasticity-based Metrics

We refer with plasticity in this work to the ability of the learner to acquire new knowledge from the current data generating distribution \mathcal{D}_k . A first measure for plasticity is the **current task accuracy** $\mathbf{A}(E_k, f_t)$ with $t \in [|T_{k-1}|, |T_k|]$. Other metrics proposed in literature are the few-shot measure *Learning Curve Area* [8] and zero-shot *Forward Transfer* [27].

Previous metrics depend on the current learning task T_k and are therefore not directly applicable to task-agnostic data streams. As the counterpart for \mathbf{WF}^w , we introduce the more generally applicable **Windowed Plasticity (WP^w)**, defined over all N evaluation tasks by the maximal accuracy *increase* $\Delta_{t,E_i}^{w,+}$ in a window of size w , similar to Eq. 3 with constraint $m < n$:

$$\mathbf{WP}_t^w = \frac{1}{N} \sum_i^N \max_n \Delta_{n,E_i}^{w,+}, \forall n \leq t \quad (5)$$

We report \mathbf{WP}^{10} and \mathbf{WP}^{100} to measure plasticity at different scales with constant space complexity.

3.2.3 Stability-Plasticity trade-off based Metrics

The main target in continual learning is to find a balance between learning new tasks T_k and retaining knowledge from previous tasks $T_{<k}$, commonly referred to as the *stability-plasticity* trade-off [15]. Stability-plasticity trade-off metrics provide a single metric to quantify this balance. The standard metric for continual learning is the **Average Accuracy (ACC)** that after learning task T_k averages

performance over all evaluation tasks: $\text{ACC}_{T_k} = \frac{1}{k} \sum_i^k \mathbf{A}(E_i, f_{T_k})$. It provides a measure of trade-off by including the accuracy of both current evaluation task E_k (plasticity) and all previous evaluation tasks $E_{<k}$ (stability). The ACC is measured only at the final model f_{T_k} and is negligent of the performance between task transitions. Therefore, we propose the **Worst-case Accuracy (WC-ACC)** as the trade-off between the accuracy on iteration t of current task T_k and the worst-case metric min-ACC $_{T_k}$ (see Eq. 2) for previous tasks:

$$\text{WC-ACC}_t = \frac{1}{k} \mathbf{A}(E_k, f_t) + (1 - \frac{1}{k}) \text{min-ACC}_{T_k} \quad (6)$$

This metric quantifies per iteration the minimal accuracy previous tasks retain after being learned, and the accuracy of the current task. WC-ACC gives a lower bound guarantee on ACC that is established over iterations. Evaluating after learning task T_k , we conclude the following lower bound:

$$\text{WC-ACC}_{|T_k|} \leq \text{ACC}_{T_k} \quad (7)$$

3.3 Tractable Continual Evaluation

The challenge in continual evaluation is twofold. First, the high evaluation frequency is computationally demanding. Second, the evaluator’s set of locally stationary test distributions may expand with the number of tasks. Furthermore, we discuss practical considerations for real-world applications by using training data for evaluation and parallelism.

Evaluation periodicity. A first relaxation for feasible continual evaluation is to increase the per-update evaluation periodicity $\rho_{eval} = 1$ to larger values. We perform an analysis for $\rho_{eval} \in \{1, 10, 10^2, 10^3\}$ on 4 benchmarks for Experience Replay (ER). We follow the full setup and datasets discussed in Section 4 and Appendix. Due to space constraints, Table 1 shows only Mini-Imagenet results as a representative subset from which we can draw the same conclusions. The full results are reported in Appendix. Important for this analysis are our findings in Section 4 showing that continual evaluation reveals catastrophic drops in performance after task transitions. Table 1 shows that these sharp drops are phased out as min-ACC and WC-ACC both increase with evaluation periodicity ρ_{eval} , and large-scale forgetting WF^{100} decreases. This phenomenon is illustrated in Figure 2, where further increasing periodicity up to the standard evaluation on task transitions ($\rho_{eval} = T_i$) becomes entirely negligent of these performance drops. Therefore, continual evaluation in the following adopts $\rho_{eval} = 1$.

Table 1: Mini-Imagenet continual evaluation metrics for a range of evaluation periodicities ρ_{eval} . Results over 5 seeds reported as mean (\pm SD).

ρ_{eval}	<i>Trade-off</i>		<i>Stability</i>		<i>Plasticity</i>	
	WC-ACC	min-ACC	WF ¹⁰	WF ¹⁰⁰	WP ¹⁰	WP ¹⁰⁰
10 ⁰	4.1 \pm 0.3	0.5 \pm 0.2	56.6 \pm 0.9	64.6 \pm 1.1	49.3 \pm 1.6	67.6 \pm 0.7
10 ¹	5.0 \pm 0.4	1.4 \pm 0.5	60.9 \pm 0.5	63.0 \pm 0.6	65.3 \pm 0.3	68.1 \pm 0.4
10 ²	6.7 \pm 0.4	3.1 \pm 0.4	58.8 \pm 0.6	60.5 \pm 0.7	67.0 \pm 0.7	67.2 \pm 0.8
10 ³	7.1 \pm 1.1	3.6 \pm 1.1	57.7 \pm 0.5	59.3 \pm 0.3	66.1 \pm 0.8	66.3 \pm 0.9

Subsampling the evaluation sets. A second relaxation for feasible continual evaluation is to control the number of evaluation samples. The set of evaluation tasks \mathcal{T}_E often grows linearly over time. This is unavoidable if we want to provide data-based performance guarantees per learned task. Nonetheless, we can reduce the absolute computation time by limiting the number of samples per evaluation set. With $\rho_{eval} = 1$ and uniformly subsampling each evaluation task’s dataset $D_{E,i}$, Table 2 indicates that a sample size of 1k provides a good approximation for using the entire test set (*All*). A smaller sample size of 100 induces more noise in the performance estimate, resulting in larger deviations compared to the entire dataset, especially notable for WF¹⁰⁰ and WP¹⁰⁰. Results for MNIST and CIFAR10 and a discussion for more complex schemes can be found in Appendix.

Exploiting training data. A disadvantage of extracting held-out evaluation data from the data stream is that this data cannot be used by the learner. Table 2 shows the continual evaluation of ER

with training subsets compared to the actual evaluation data, with similar ACC of 31.5 ± 0.5 for the train set and even slightly higher 32.7 ± 1.3 for the test set. We find that worst-case stability metric min-ACC is very similar on both sets, and catastrophic forgetting in WF^{100} is significantly higher for the training data. This suggests it can serve as a good (over)estimator to monitor the stability of the learner.

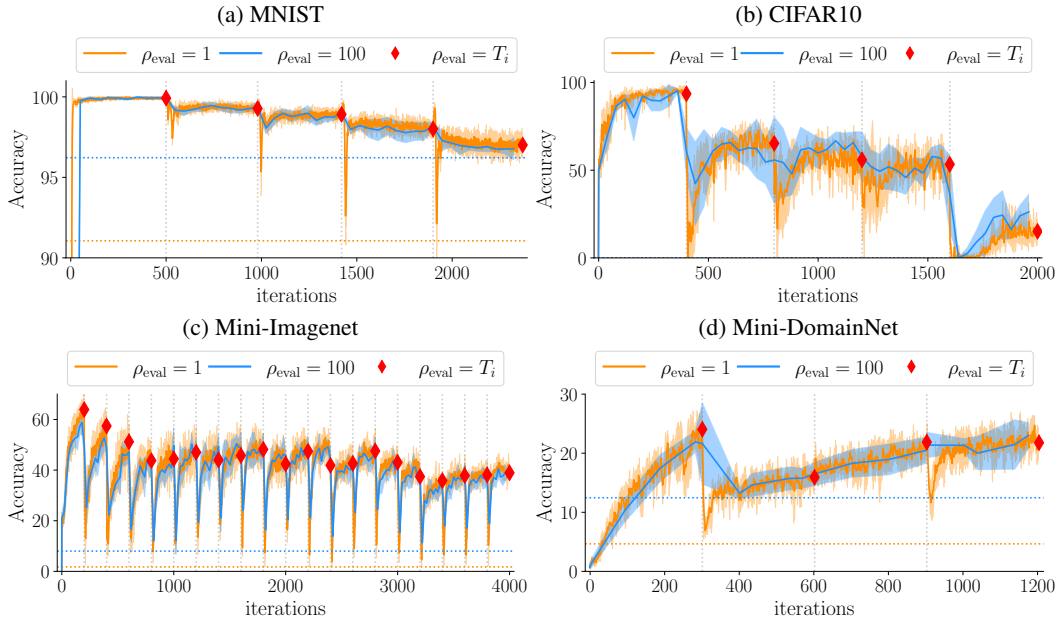
Parallelism. In real-world continual evaluation, parallelism can be exploited by separating the *learner* and *evaluator* in different processing units. The evaluator captures a snapshot from the model for evaluation, while the learner continues the continual optimization process. In this scenario, the periodicity ρ_{eval} is dependent on the evaluator’s processing time.

Table 2: Mini-Imagenet continual evaluation metrics for different subsample sizes of the evaluation sets and comparison to training set performance with $\rho_{eval} = 1$. ‘All’ indicates the full task test sets. Results over 5 seeds reported as mean (\pm SD).

		<i>Trade-off</i>		<i>Stability</i>		<i>Plasticity</i>	
	Sample size	WC-ACC	min-ACC	WF ¹⁰	WF ¹⁰⁰	WP ¹⁰	WP ¹⁰⁰
Eval	All	4.1 ± 0.3	0.5 ± 0.2	56.0 ± 0.7	64.2 ± 0.6	48.3 ± 1.8	67.8 ± 0.4
	10^3	4.1 ± 0.3	0.5 ± 0.2	56.6 ± 0.9	64.6 ± 1.1	49.3 ± 1.6	67.6 ± 0.7
	10^2	3.9 ± 0.5	0.3 ± 0.2	60.8 ± 2.0	71.6 ± 0.7	51.5 ± 2.7	74.3 ± 0.7
Train	10^3	5.4 ± 0.2	0.5 ± 0.2	73.8 ± 0.3	79.9 ± 0.3	50.4 ± 1.9	78.0 ± 0.5

4 Identifying the stability gap with continual evaluation

Figure 2: Accuracy curves for the first task of Experience Replay. Evaluation periodicity ranges from standard evaluation on task transitions ($\rho_{eval} = T_i$) to per-iteration continual evaluation ($\rho_{eval} = 1$), reported as mean (\pm SD) over 5 seeds. Per-iteration evaluation reveals sharp, transient drops in performance when learning new tasks, i.e. the *stability gap*. Horizontal lines indicate the min-ACC averaged over seeds.



We start by conducting an empirical study confined to Experience Replay (ER) [9], as it has been shown to prevail over regularization based methods especially for class and domain incremental learning [38, 27, 8]. ER stores a small subset of samples in a memory buffer, which are revisited later on by

sampling mini-batches that are partly new data, partly memory data. Due to its simplicity and effectiveness against catastrophic forgetting, it has been widely adopted in literature [34, 9, 11, 7]. We focus on class and domain incremental learning, which have been shown to exhibit significant forgetting with gradient-based learning [18, 38], which we additionally confirmed with experiments in Appendix.

Datasets. For class incremental learning, sets of new classes are observed sequentially. We examine three standard benchmarks based on MNIST, CIFAR10, and Mini-Imagenet and split their data in 5, 5, and 20 tasks based on their 10, 10, and 100 classes respectively. **MNIST** [24] consists of grayscale handwritten digits, **CIFAR10** [22] contains images from a range of vehicles and animals, and **Mini-Imagenet** [40] is a 100-class subset of Imagenet [36]. For domain incremental learning we consider drastic domain changes in **Mini-DomainNet** [42], a scaled-down subset of 126 classes of DomainNet [32] with over 90k images, considering domains: clipart, painting, real, sketch.

Setup. We employ continual evaluation with $\rho_{\text{eval}} = 1$ and subset size 1k per evaluation task, based on our feasibility analysis in Section 3.3. For reference with literature, task-transition based metrics ACC and FORG follow standard evaluation with the entire test set. MNIST uses an MLP with 2 hidden layers of 400 units. CIFAR10, Mini-Imagenet and Mini-DomainNet use a slim version of Resnet18 [27, 11]. SGD optimization is used with 0.9 momentum. To make sure our worst-case analysis applies to the best-case configuration for ER, we run a gridsearch over different hyperparameters and select the entry with the highest stability-plasticity trade-off metric ACC on the held-out evaluation data [27]. Details for all experiments can be found in Appendix. We will provide the full codebase for reproducibility.

Analysis with continual evaluation. Figure 2 illustrates the first task accuracy curves for ER over the 4 benchmarks. The red markers on task transitions ($\rho_{\text{eval}} = T_i$) indicate the standard evaluation scheme in continual learning. We find that continual evaluation ($\rho_{\text{eval}} = 1$) reveals significant temporary forgetting between task transitions, both for the class and domain incremental benchmarks. After the significant performance drops, partial recovery follows, making the task-transition based metrics such as ACC and FORG bad worst-case performance estimators. We refer to this *phenomenon of transient, significant forgetting when learning new tasks* as the **stability gap**.

4.1 Conceptual analysis of the stability gap

Our empirical findings suggest the significant drops in accuracy occur directly after the task-transition, as shown in Figure 2. To establish a conceptual grounding for this phenomenon, we first disentangle the continual learning gradients of the objective \mathcal{L} in α -weighed plasticity and stability gradients

$$\nabla \mathcal{L} = \alpha \nabla \mathcal{L}_{\text{plasticity}} + (1 - \alpha) \nabla \mathcal{L}_{\text{stability}} \quad (8)$$

In gradient-based optimization of model $f_{t,\theta}$, $\nabla \mathcal{L}_{\text{plasticity}}$ improves performance on the current task and $\nabla \mathcal{L}_{\text{stability}}$ maintains performance on past tasks. In the viewpoint of the stability-plasticity trade-off [15], continual learning methods aim to balance both gradient terms. However, due to task-oriented evaluation and lack of continual evaluation, progress in this balance has only been verified on the task-transitions.

We consider the initial learning steps when starting to train on a new task, where the loss on that task tends to be high with large gradient norm $\|\nabla \mathcal{L}_{\text{plasticity}}\|$. Following Eq. 8, this would result in greedy updates when $\|\nabla \mathcal{L}_{\text{stability}}\|$ is small, sacrificing performance on past tasks in favour of large gains on the new task. In the following, we hypothesize this is the case for various continual learning methods due to potential conceptual shortcomings on task transitions and find supporting empirical evidence. Assuming later in the learning process, the new task loss $\mathcal{L}_{\text{plasticity}}$ starts to plateau, better matching norms of both gradient terms might enable recovering performance on old tasks that was lost during the initial greedy updates.

Finetuning optimizes solely for the current task T_k and is not concerned with stability, with $\|\nabla \mathcal{L}_{\text{stability}}\| = 0$. Using the continual evaluation framework, we observe that severe forgetting of past tasks occurs already during the first few training iterations on a new task (see Appendix). This confirms that updates based on $\nabla \mathcal{L}_{\text{plasticity}}$ are greedy early on learning a new task.

Experience replay learns concurrently from data of the new task and a subset of previous task data sampled from experience buffer \mathcal{M} . The loss term $\mathcal{L}_{\text{stability}}$ is obtained by revisiting previous task

samples in \mathcal{M} . To establish whether the gradient norm of this loss term is indeed low during the early phase of training on a new task, we first consider a data stream with two subsequent tasks. When training starts on T_2 , $f_{t,\theta}$ presumably has converged for the first task T_1 , resulting in $\|\nabla \mathcal{L}_{T_1}\| \approx 0$. Therefore, directly after the task transition, we indeed have $\|\nabla \mathcal{L}_{\text{stability}}\| \approx 0$ because the replayed samples are exclusively from T_1 . Generalizing this to longer task sequences requires not only nearly-zero gradients for the previous task, but for all previous task data in the entire replay buffer \mathcal{M} . This has been empirically confirmed by Verwimp et al. [39] indicating ER to consistently converge to near-zero gradients for \mathcal{M} . We demonstrate similar findings for MNIST in Figure 3(e-h).

4.2 Finding a stability gap in other continual learning methods

In this section, we examine whether the stability gap can be observed for other representative methods in continual learning. We focus on GEM [27], and *regularization-based methods* [10] which can be subdivided in two families based on how they define the regularization objective $\mathcal{L}_{\text{stability}}$. The details for the experiments are detailed in Appendix.

Gradient-constrained replay. Gradient Episodic memory (GEM) [27] exploits a memory buffer \mathcal{M} similar to ER, divided over K equally sized task buffers \mathcal{M}_k . However, instead of directly optimizing the objective for the samples in \mathcal{M} , their task-specific gradients $g_k = \nabla \mathcal{L}(\mathcal{M}_k)$ are used to compose a set of constraints. The constraints $\langle g_t, g_n \rangle \geq 0, \forall n < k$ attempt to prevent loss increase on the $k-1$ previous tasks, with $g_t = \nabla \mathcal{L}_{\text{plasticity}}$ the gradient of the current observed sample $(x, y)_t$ in task T_k . Current gradient g_t is projected to the closest gradient \tilde{g} satisfying the constraint set, obtained by Quadratic Programming. We reformulate the projection to obtain the conditional stability gradient:

$$\nabla \mathcal{L}_{\text{stability}} = \begin{cases} \vec{0}, & \text{if } \langle g_t, g_n \rangle \geq 0, \forall n < k \\ \tilde{g} - g_t, & \text{otherwise} \end{cases} \quad (9)$$

As the GEM constraints explicitly attempt to prevent increase in previous task losses, $\|\nabla \mathcal{L}_{\text{stability}}\|$ is only zero if the current gradient update g_t lies within the feasible region of the constraint set or is near-zero with only slightly violated constraints $\|\tilde{g} - g_t\| \approx 0$. As in the dot-product constraints the sign is determined solely based on the gradient angles, satisfying them is independent of the norm of $\|\nabla \mathcal{L}_{\text{stability}}\|$ on task transitions. This suggests that GEM might enable avoiding or alleviating the stability gap.

However, empirically we find that also GEM is prone to the stability gap (Figure 3). Compared to ER, the stability gap of GEM is significantly larger, indicated by the large discrepancy in the horizontal lines representing average min-ACC. On the task transitions for MNIST, Figure 3(e-h) shows that GEM has significant $\|\nabla \mathcal{L}_{\text{stability}}\|$ compared to ER (determined following Eq. 9), indicating large violations of the constraints. However, especially for task transitions T_3 and T_4 we observe the gradients to drop to near-zero magnitude, resulting in a few updates mostly based on $\nabla \mathcal{L}_{\text{plasticity}}$.

Distillation-based methods [37, 25, 33] extract the model distribution directly from the previous task model $f_{T_{k-1}}$, using the currently available data from T_k . The current task distribution is then prone to matching the previous one, by means of knowledge distillation [17]. At the first iteration on a new task, both the previous task model and the current model are identical, leading to $\|\nabla \mathcal{L}_{\text{stability}}\| = 0$ caused by perfectly matching distributions. This suggests that distillation-based methods might also suffer from the stability gap.

Empirically we indeed find a stability gap for Learning without Forgetting (LwF) [25] in the domain incremental Mini-DomainNet (Figure 4). The stability gaps are especially notable for T_1 and T_2 in Figure 4(a,b). Figure 4(e-g) indicate the zero gradient norms on task transitions.

Model-prior based methods [21, 41, 2, 20] typically have $\mathcal{L}_{\text{stability}} = \Omega \|\theta_t - \theta_{|T_{k-1}|}\|_2^2$ with parameters $\theta_t \in \mathbb{R}^M$ and penalty matrix $\Omega \in \mathbb{R}^{M \times M}$. Important parameters of previous tasks have larger penalization to avoid forgetting. Directly after a task transition, the parameters of the current model $f_{t,\theta}$ are exactly equal to the previous task model $f_{|T_{k-1}|,\theta}$, leading to a perfectly satisfied regularization objective with $\|\nabla \mathcal{L}_{\text{stability}}\| = 0$. This suggests the stability gap might also affect model-prior based methods.

Performing the same experiments for EWC [21] as for LwF on domain incremental Mini-DomainNet, our results show that EWC performs only marginally better than finetuning in terms of ACC, and on

Figure 3: GEM and ER accuracy curves (a-d) on MNIST for the first four tasks, and the per-iteration L2-norms of current $\nabla\mathcal{L}_{\text{stability}}$ (e-h). Results reported as mean (\pm SD) over 5 seeds, with horizontal lines representing average min-ACC. Vertical lines indicate the start of a new task. Note that the x-axis scale varies over (a-d) and (e-h) are zooms of the first 50 iterations.

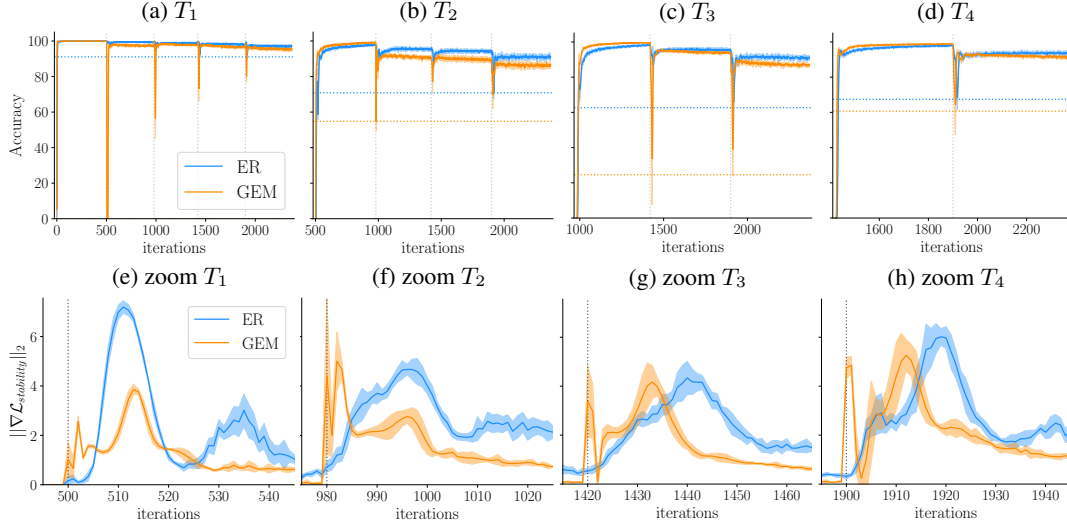
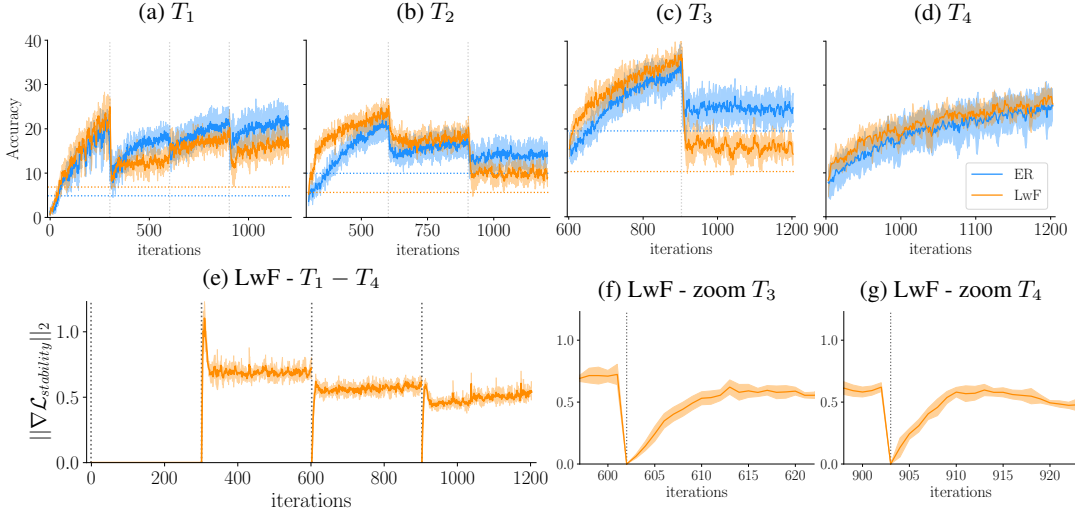


Figure 4: LwF and ER accuracy curves (a-d) on Mini-DomainNet for the four domains, and the per-iteration L2-norms of current $\nabla\mathcal{L}_{\text{stability}}$ (e-g). Results are reported as mean (\pm SD) over 5 seeds, with horizontal lines representing average min-ACC. Vertical lines indicate the start of a new task. Note that the x-axis scale varies over (a-d), (e) overviews the full learning trajectory, and (f,g) are zooms in on the first few iterations for the last two tasks.



par in terms of worst-case min-ACC. The ineffectiveness of model-prior methods in this setting has been suggested in previous work [38, 35, 18], and therefore inhibits obtaining further evidence for the stability gap. Continual evaluation metrics and plots are reported in Appendix.

5 Conclusion

In this work, we first identified shortcomings of the standard sparse evaluation protocol for task-based continual learning and proposed a novel framework for per-iteration *continual evaluation*. To enable measuring worst-case performance for continual learning and applicability to task-agnostic

data streams, we proposed a set of novel evaluation metrics. Using this evaluation framework, we identified a striking and potentially problematic phenomenon: the stability gap. In a variety of settings, we showed that upon starting to learn a new task, various commonly used continual learning methods suffer from a significant loss in performance on previously learned tasks that, intriguingly, is often recovered later on. Such transient forgetting, which has remained unidentified so far, can be problematic in real-world applications. In future work it would be interesting to search for, or develop, continual learning methods that can overcome the stability gap. Another intriguing question raised by this work is whether the stability gap also applies to biological neural networks: when learning something new, does the brain suffer from transient forgetting as well?

Acknowledgments and Disclosure of Funding

The authors were funded by ERC project 101021347 KeepOnLearning and the KULeuven C1 project Macchina.

References

- [1] Achille, A., Lam, M., Tewari, R., Ravichandran, A., Maji, S., Fowlkes, C. C., Soatto, S., and Perona, P. (2019). Task2vec: Task embedding for meta-learning. In *Proceedings of the IEEE/CVF International Conference on Computer Vision (ICCV)*.
- [2] Aljundi, R., Babiloni, F., Elhoseiny, M., Rohrbach, M., and Tuytelaars, T. (2018). Memory aware synapses: Learning what (not) to forget. In *ECCV*, pages 139–154.
- [3] Aljundi, R., Caccia, L., Belilovsky, E., Caccia, M., Lin, M., Charlin, L., and Tuytelaars, T. (2019a). Online continual learning with maximally interfered retrieval. *Proceedings NeurIPS 2019*, 32.
- [4] Aljundi, R., Lin, M., Goujaud, B., and Bengio, Y. (2019b). Gradient based sample selection for online continual learning. *NeurIPS*, pages 11816–11825.
- [5] Caccia, L., Aljundi, R., Asadi, N., Tuytelaars, T., Pineau, J., and Belilovsky, E. (2022). New insights on reducing abrupt representation change in online continual learning. In *International Conference on Learning Representations*.
- [6] Caccia, M., López, P. R., Ostapenko, O., Normandin, F., Lin, M., Page-Caccia, L., Laradji, I. H., Rish, I., Lacoste, A., Vázquez, D., and Charlin, L. (2020). Online fast adaptation and knowledge accumulation (osaka): a new approach to continual learning. In *NeurIPS*.
- [7] Chaudhry, A., Dokania, P. K., Ajanthan, T., and Torr, P. H. (2018). Riemannian walk for incremental learning: Understanding forgetting and intransigence. In *ECCV*, pages 532–547.
- [8] Chaudhry, A., Ranzato, M., Rohrbach, M., and Elhoseiny, M. (2019a). Efficient lifelong learning with a-GEM. In *International Conference on Learning Representations*.
- [9] Chaudhry, A., Rohrbach, M., Elhoseiny, M., Ajanthan, T., Dokania, P. K., Torr, P. H., and Ranzato, M. (2019b). Continual learning with tiny episodic memories. *arXiv preprint arXiv:1902.10486*.
- [10] De Lange, M., Aljundi, R., Masana, M., Parisot, S., Jia, X., Leonardis, A., Slabaugh, G., and Tuytelaars, T. (2021). A continual learning survey: Defying forgetting in classification tasks. *IEEE Transactions on Pattern Analysis and Machine Intelligence*, pages 1–1.
- [11] De Lange, M. and Tuytelaars, T. (2021). Continual prototype evolution: Learning online from non-stationary data streams. In *Proceedings of the IEEE/CVF International Conference on Computer Vision*, pages 8250–8259.
- [12] Devlin, J., Chang, M.-W., Lee, K., and Toutanova, K. (2018). Bert: Pre-training of deep bidirectional transformers for language understanding. *arXiv preprint arXiv:1810.04805*.
- [13] French, R. M. (1999). Catastrophic forgetting in connectionist networks. *Trends in cognitive sciences*, 3(4):128–135.
- [14] Goodfellow, I. J., Mirza, M., Xiao, D., Courville, A., and Bengio, Y. (2013). An empirical investigation of catastrophic forgetting in gradient-based neural networks. *arXiv preprint arXiv:1312.6211*.

- [15] Grossberg, S. (1982). *Studies of mind and brain : neural principles of learning, perception, development, cognition, and motor control*. Boston studies in the philosophy of science 70. Reidel, Dordrecht.
- [16] Hayes, T. L., Cahill, N. D., and Kanan, C. (2019). Memory efficient experience replay for streaming learning. In *2019 International Conference on Robotics and Automation (ICRA)*, pages 9769–9776. IEEE.
- [17] Hinton, G., Vinyals, O., and Dean, J. (2015). Distilling the knowledge in a neural network. *arXiv preprint arXiv:1503.02531*.
- [18] Hsu, Y.-C., Liu, Y.-C., and Kira, Z. (2018). Re-evaluating continual learning scenarios: A categorization and case for strong baselines. *arXiv preprint arXiv:1810.12488*.
- [19] Hull, J. (1994). A database for handwritten text recognition research. *IEEE Transactions on Pattern Analysis and Machine Intelligence*, 16(5):550–554.
- [20] Kao, T.-C., Jensen, K., van de Ven, G., Bernacchia, A., and Hennequin, G. (2021). Natural continual learning: success is a journey, not (just) a destination. In Ranzato, M., Beygelzimer, A., Dauphin, Y., Liang, P., and Vaughan, J. W., editors, *Advances in Neural Information Processing Systems*, volume 34, pages 28067–28079. Curran Associates, Inc.
- [21] Kirkpatrick, J., Pascanu, R., Rabinowitz, N., Veness, J., Desjardins, G., Rusu, A. A., Milan, K., Quan, J., Ramalho, T., Grabska-Barwinska, A., et al. (2017). Overcoming catastrophic forgetting in neural networks. *PNAS*, page 201611835.
- [22] Krizhevsky, A., Hinton, G., et al. (2009). Learning multiple layers of features from tiny images.
- [23] Krizhevsky, A., Sutskever, I., and Hinton, G. E. (2012). Imagenet classification with deep convolutional neural networks. In Pereira, F., Burges, C., Bottou, L., and Weinberger, K., editors, *Advances in Neural Information Processing Systems*, volume 25. Curran Associates, Inc.
- [24] LeCun, Y. and Cortes, C. (2010). MNIST handwritten digit database.
- [25] Li, Z. and Hoiem, D. (2017). Learning without forgetting. *IEEE transactions on pattern analysis and machine intelligence*, 40(12):2935–2947.
- [26] Lomonaco, V., Pellegrini, L., Cossu, A., Carta, A., Graffieti, G., Hayes, T. L., De Lange, M., Masana, M., Pomponi, J., van de Ven, G. M., et al. (2021). Avalanche: an end-to-end library for continual learning. In *Proceedings of the IEEE/CVF Conference on Computer Vision and Pattern Recognition*, pages 3600–3610.
- [27] Lopez-Paz, D. and Ranzato, M. (2017). Gradient episodic memory for continual learning. In *Advances in neural information processing systems*, pages 6467–6476.
- [28] Masana, M., Liu, X., Twardowski, B., Menta, M., Bagdanov, A. D., and van de Weijer, J. (2020). Class-incremental learning: survey and performance evaluation. *arXiv preprint arXiv:2010.15277*.
- [29] Mnih, V., Kavukcuoglu, K., Silver, D., Graves, A., Antonoglou, I., Wierstra, D., and Riedmiller, M. (2013). Playing atari with deep reinforcement learning. *arXiv preprint arXiv:1312.5602*.
- [30] Netzer, Y., Wang, T., Coates, A., Bissacco, A., Wu, B., and Ng, A. Y. (2011). Reading digits in natural images with unsupervised feature learning.
- [31] Paszke, A., Gross, S., Massa, F., Lerer, A., Bradbury, J., Chanan, G., Killeen, T., Lin, Z., Gimelshein, N., Antiga, L., Desmaison, A., Kopf, A., Yang, E., DeVito, Z., Raison, M., Tejani, A., Chilamkurthy, S., Steiner, B., Fang, L., Bai, J., and Chintala, S. (2019). Pytorch: An imperative style, high-performance deep learning library. In Wallach, H., Larochelle, H., Beygelzimer, A., d'Alché-Buc, F., Fox, E., and Garnett, R., editors, *Advances in Neural Information Processing Systems 32*, pages 8024–8035. Curran Associates, Inc.
- [32] Peng, X., Bai, Q., Xia, X., Huang, Z., Saenko, K., and Wang, B. (2019). Moment matching for multi-source domain adaptation. In *Proceedings of the IEEE International Conference on Computer Vision*, pages 1406–1415.
- [33] Rannen, A., Aljundi, R., Blaschko, M. B., and Tuytelaars, T. (2017). Encoder based lifelong learning. In *ICCV*, pages 1320–1328.
- [34] Rebuffi, S.-A., Kolesnikov, A., Sperl, G., and Lampert, C. H. (2017). icarl: Incremental classifier and representation learning. In *CVPR*, pages 2001–2010.
- [35] Riemer, M., Cases, I., Ajemian, R., Liu, M., Rish, I., Tu, Y., , and Tesauro, G. (2019). Learning to learn without forgetting by maximizing transfer and minimizing interference. In *International Conference on Learning Representations*.

- [36] Russakovsky, O., Deng, J., Su, H., Krause, J., Satheesh, S., Ma, S., Huang, Z., Karpathy, A., Khosla, A., Bernstein, M., et al. (2015). Imagenet large scale visual recognition challenge. *IJCV*, 115(3):211–252.
- [37] Silver, D. L. and Mercer, R. E. (2002). The task rehearsal method of life-long learning: Overcoming impoverished data. In *Conference of the Canadian Society for Computational Studies of Intelligence*, pages 90–101. Springer.
- [38] van de Ven, G. M. and Tolias, A. S. (2019). Three scenarios for continual learning. *arXiv preprint arXiv:1904.07734*.
- [39] Verwimp, E., De Lange, M., and Tuytelaars, T. (2021). Rehearsal revealed: The limits and merits of revisiting samples in continual learning. In *Proceedings of the IEEE/CVF International Conference on Computer Vision (ICCV)*, pages 9385–9394.
- [40] Vinyals, O., Blundell, C., Lillicrap, T., Kavukcuoglu, K., and Wierstra, D. (2016). Matching networks for one shot learning. In *Proceedings of the 30th International Conference on Neural Information Processing Systems*, pages 3637–3645.
- [41] Zenke, F., Poole, B., and Ganguli, S. (2017). Continual learning through synaptic intelligence. In *ICML*, pages 3987–3995. JMLR. org.
- [42] Zhou, K., Yang, Y., Qiao, Y., and Xiang, T. (2021). Domain adaptive ensemble learning. *IEEE Transactions on Image Processing*, 30:8008–8018.

Appendix

Supplemental materials include a discussion on the limitations and societal impact of this work (Appendix A), the detailed reproducibility details for all experiments (Appendix B), and additional empirical evidence in Appendix C.

Appendix C provides additional results for 1) a benchmark analysis of worst-case forgetting with finetuning; 2 and 3) evaluation periodicity and subsampling the evaluation sets for tractable continual evaluation; 4) EWC on Mini-DomainNet; 5) GEM on MNIST and CIFAR10; and 6) a partial loss analysis for MNIST and CIFAR10.

A Limitations and societal impact

Computational complexity. Both time and space complexity are important factors for continual learning with constrained resources. The space complexity for continual evaluation retains a linear increase with the number of tasks k as for standard evaluation. However, the time complexity changes from a task-based periodicity to a per-iteration periodicity. The ratio of computational increase for a single task T_k can be defined as $\frac{|T_k| - |T_{k-1}|}{\rho_{\text{eval}}}$ where $|T_k| - |T_{k-1}|$ is the number of iterations for that task. Albeit the increase in time complexity, due to our empirical findings, we advocate the use of continual evaluation when possible for analysis of the learning behavior and especially for safety-critical applications. We refer to Section 3.3 to enable tractable continual evaluation.

Societal impact. A continual learning agent operational in the real world may lead to unpredictable results as the agent may observe malicious data points, learn from highly biased data, or learn undesirable behavior that diverges from its original goals. Such evolution can remain undetected with sparse or even no evaluation of the learner. Therefore, we deem continual evaluation important for a fine-grained monitoring of the agent’s learning behavior.

B Reproducibility details

Datasets and transforms. For class incremental learning, MNIST, CIFAR10, and Mini-Imagenet and split their data in 5, 5, and 20 tasks based on their 10, 10, and 100 classes respectively. Each set of data associated to a set of classes then constitutes a task. This split is performed for both the training and test sets, to create a training and evaluation stream of sequential tasks. The order of the class-groupings to create tasks is sequential, e.g. in MNIST we use the digits $\{0, 1\}$ for T_1 , $\{2, 3\}$ for T_2 , up to $\{8, 9\}$ for T_5 . **MNIST** [24] consists of grayscale handwritten digits with (28×28) inputs. The dataset contains about 70k images from which 60k training and 10k test images. **CIFAR10** [22] contains 50k training and 10k test images from a range of vehicles and animals with colored (32×32) inputs. **Mini-Imagenet** [40] is a 100-class subset of Imagenet [36], with colored inputs resized to (84×84) . Each class contains 600 images, from which 500 are used for training and 100 for testing. For domain incremental learning we consider drastic domain changes in **Mini-DomainNet** [42], a scaled-down

subset of 126 classes of DomainNet [32] with over 90k images, considering domains: clipart, painting, real, sketch. Inputs from all datasets are normalized and Mini-DomainNet resizes the original DomainNet images with their smaller size to 96 using bilinear interpolation, followed by a center crop to fixed $(3 \times 96 \times 96)$ inputs. For all datasets, all used transforms are deterministic.

Gridsearch procedure. All experiments for MNIST and CIFAR10 perform a gridsearch over hyperparameters, with each run averaged over 5 initialization seeds. The result with highest ACC is selected as best entry, following [27]. For computational feasibility in the larger benchmarks, Mini-Imagenet and Mini-DomainNet, the gridsearch is performed over a single seed and the top entry is averaged over 5 initialization seeds. For all experiments, the learning rate η for the gradient-based updates is considered as hyperparameter in the set $\eta \in \{0.1, 0.01, 0.001, 0.0001\}$. A fixed batch size is used for all benchmarks, with 128 for the larger-scale Mini-Imagenet and Mini-DomainNet, and 256 for the smaller MNIST and CIFAR10. Method-specific and other continual learning hyperparameters are discussed below.

Continual evaluation setup. We employ continual evaluation with $\rho_{\text{eval}} = 1$ and subset size 1k per evaluation task, based on our feasibility analysis in Section 3.3. For reference with literature, task-transition based metrics ACC and FORG follow standard evaluation with the entire test set.

Architectures and optimization. MNIST uses an MLP with 2 hidden layers of 400 units. CIFAR10, Mini-Imagenet and Mini-DomainNet use a slim version of Resnet18 [27, 11]. SGD optimization is used with 0.9 momentum. MNIST, CIFAR10 and Mini-Imagenet are configured for 10 epochs per task, which roughly equals to 500, 400, and 200 iterations per task with the defined batch sizes. Mini-DomainNet has 300 training iterations per task to balance compute equally over the tasks.

Results for identifying the stability gap in Section 4(intro) are obtained using Experience Replay (ER) where we consider the loss weighing hyperparameter $\alpha \in \{0.1, 0.3, 0.5, 0.7, 0.9\}$ as in Eq. 8. The above defined batch size indicates the number of new samples in the mini-batch. Additionally, another batch of the same size is sampled from the replay memory, which is concatenated to the new data, following [9, 39]. To determine which samples are selected for storage in the buffer, class-based reservoir sampling is used as in [11]. We indicate the selected hyperparameters (η, α) per dataset here: MNIST (0.01, 0.3), CIFAR10 (0.1, 0.7), Mini-Imagenet (0.1, 0.5), Mini-DomainNet (0.1, 0.3).

Results in Section 3.3 are based on the best ACC results for ER reported in Section 4, see above for details. In the experiment for different subsample sizes, the evaluation and training subsets are obtained from the entire set through a uniform sampling per evaluation.

Results in Section 4.2 use the ER results obtained from Section 4(intro). **LwF** [25] is configured with a standard softmax temperature of 2 as proposed by the authors and previous work [25, 17]. The best learning rate for Mini-Domainnet was $\eta = 0.01$. **GEM** [27] uses the author’s standard bias parameter of 0.5, with best learning rates $\eta = 0.01$ and $\eta = 0.001$ for MNIST and CIFAR10 respectively. **EWC** for Mini-DomainNet we had to perform gridsearch to find solution with performance better than or on par with finetuning. The best configuration had $\eta = 0.01$ and regularization strength $\lambda = 1$, out of $\lambda = \{0.1, 1, 10, 100, 1000\}$.

Used codebases and equipment. The experiments were based on the Avalanche framework [26] in Pytorch [31]. All results were performed on a compute cluster with a range of NVIDIA GPU’s.

C Additional Results

C.1 Benchmark analysis of worst-case forgetting with finetuning

This section examines the worst-case performance for the three continual learning scenarios: task, class, and domain incremental learning. We examine **finetuning** as a standard gradient-based learning method with stochastic gradient descent, repeatedly shown to be prone to catastrophic forgetting and therefore the standard baseline for worst-case performance in continual learning [10, 38].

Additional Datasets. We examine 3 additional domain incremental benchmarks. Two benchmarks are based on transforming MNIST per task, with either a fixed random permutations per task in **Permuted-MNIST** [14] and a rotation transform in **Rotated-MNIST** [27]. **Digits** contains a sequence of digits datasets: MNIST, SVHN [30], USPS [19].

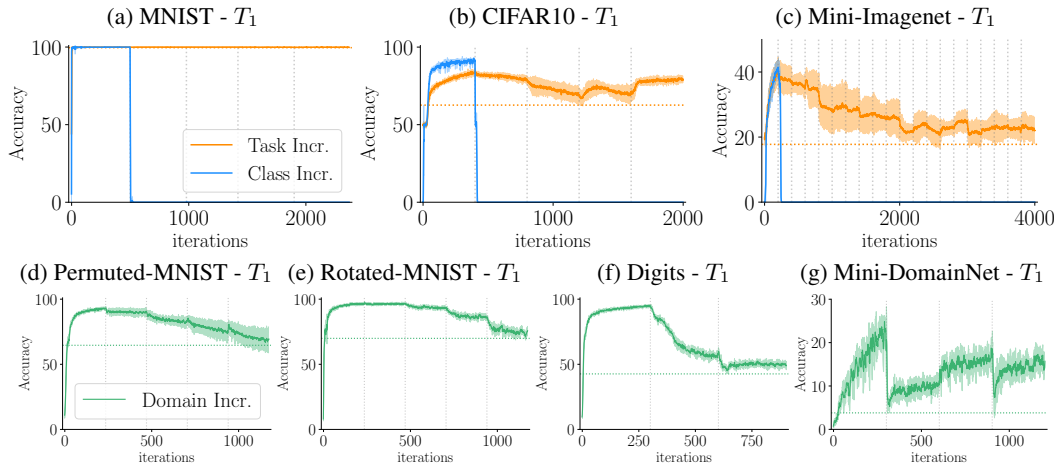
Experiment setup. All digit-based experiments use an MLP with 2 hidden layers of 400 units. CIFAR10, Mini-Imagenet and Mini-DomainNet use a slim version of Resnet18 as in [27, 11]. SGD optimization is used with 0.9 momentum.

Worst-case analysis. Our analysis aims to identify scenarios where measuring worst-case performance is crucial for a continual learner. We can identify these settings when significant forgetting occurs even in the best-possible configuration for the worst-case baseline. Therefore, we perform a gridsearch for finetuning and select the entry with best worst-case performance (WC-ACC). Comparing the **class and task incremental** settings, the three benchmarks in Figure 5(a-c) clearly illustrate catastrophic forgetting for the class incremental setup, whereas task incremental retains significant performance for this baseline. This becomes clear in the continual evaluation results from the min-ACC in Table 3 which is zero for all class incremental runs, whereas task incremental retains 97.2, 60.5, 30.0% for MNIST, CIFAR10 and Mini-Imagenet respectively. In the four **domain incremental** learning setups in Figure 5(d-g), the MNIST-based and Digits benchmarks forget only gradually with finetuning compared to the coarse domain shifts and sharp drops in accuracy in Mini-DomainNet. This is indicated by the high WF^{10} and WF^{100} for Mini-DomainNet in Table 3. In the main paper, we examine the setting with most severe catastrophic forgetting, i.e. class-incremental MNIST, CIFAR10, Mini-Imagenet, and domain-incremental Mini-DomainNet.

Table 3: Finetuning results with continual evaluation for 7 benchmarks in class, task and domain incremental learning. Results are reported as mean (\pm SD) over 5 seeds.

	<i>Trade-off</i>		<i>Stability</i>				<i>Plasticity</i>	
	ACC	WC-ACC	min-ACC	FORG	WF^{10}	WF^{100}	WP^{10}	WP^{100}
Class Incr.								
MNIST	19.5 \pm 0.1	19.7 \pm 0.1	0.0 \pm 0.0	99.7 \pm 0.1	86.1 \pm 3.5	86.3 \pm 3.6	77.8 \pm 4.4	96.9 \pm 3.4
CIFAR10	17.8 \pm 0.6	17.8 \pm 0.5	0.0 \pm 0.0	85.7 \pm 0.8	46.6 \pm 2.5	72.4 \pm 0.6	62.0 \pm 1.9	83.8 \pm 1.5
Mini-Imagenet	3.3 \pm 0.1	3.3 \pm 0.1	0.0 \pm 0.0	54.9 \pm 0.5	28.4 \pm 0.8	52.9 \pm 0.6	29.2 \pm 1.5	52.8 \pm 0.8
Task Incr.								
MNIST	98.3 \pm 1.0	97.6 \pm 1.0	97.2 \pm 1.3	1.7 \pm 1.2	3.5 \pm 2.6	4.1 \pm 2.5	40.3 \pm 3.3	44.2 \pm 3.4
CIFAR10	70.4 \pm 1.7	65.3 \pm 1.8	60.5 \pm 2.4	12.5 \pm 3.1	5.6 \pm 0.1	10.9 \pm 2.4	10.6 \pm 1.1	27.8 \pm 2.0
Mini-Imagenet	36.7 \pm 3.6	31.9 \pm 2.3	30.0 \pm 2.4	21.6 \pm 4.3	6.4 \pm 1.1	12.9 \pm 2.1	11.6 \pm 1.0	33.6 \pm 1.5
Domain Incr.								
Permuted-MNIST	84.6 \pm 1.9	82.2 \pm 1.8	79.0 \pm 2.3	12.2 \pm 2.4	5.5 \pm 0.3	8.9 \pm 1.3	57.2 \pm 1.8	81.0 \pm 0.3
Rotated-MNIST	91.0 \pm 1.1	87.4 \pm 0.8	84.8 \pm 1.1	7.9 \pm 1.4	6.3 \pm 1.3	8.9 \pm 0.6	16.9 \pm 0.5	21.4 \pm 0.3
Digits	57.6 \pm 0.3	56.6 \pm 0.4	46.2 \pm 0.6	14.1 \pm 0.8	6.2 \pm 0.7	10.6 \pm 0.8	17.9 \pm 1.3	39.6 \pm 1.5
Mini-DomainNet	15.1 \pm 1.2	10.2 \pm 1.3	4.9 \pm 1.3	13.4 \pm 1.9	16.7 \pm 1.2	19.6 \pm 1.1	10.5 \pm 0.9	16.9 \pm 1.2

Figure 5: Finetuning results for the first task of 7 benchmarks, reported as mean (\pm SD) over 5 seeds. Horizontal lines indicate the min-ACC averaged over seeds.



C.2 Tractable continual evaluation: Evaluation periodicity

For the Mini-Imagenet ER results in Section 3.3, we additionally report the results for MNIST, CIFAR10, and Mini-DomainNet in Table 4. We find consistent conclusions as for Mini-Imagenet discussed in the main paper, i.e. the stability gap is unobserved for larger evaluation periodicity, especially notable for $\rho_{eval} \in \{100, 1000\}$ which are indicated in bold. The subsample size of the evaluation sets is 1000 as for the other experiments in this work.

We noticed that results in CIFAR10 have large variance in min-ACC (and hence WC-ACC) for $\rho_{eval} = 100$. As the CIFAR10 accuracy is noisy over the iterations as indicated in Figure 2, we found in some runs for $\rho_{eval} = 100$ to completely miss the accuracy drop to zero on T_4 for 2 out of the 5 seeds. This dependency on initialization seed stresses the importance of smaller ρ_{eval} to reduce dependency on the exact point of evaluation.

Table 4: Full results on MNIST, CIFAR10, Mini-Imagenet and Mini-DomainNet in continual evaluation metrics for a range of evaluation periodicities ρ_{eval} . Results over 5 seeds reported as mean (\pm SD). The Mini-Imagenet subset of the full results is reported in the main paper in Table 1.

ρ_{eval}	<i>Trade-off</i>		<i>Stability</i>		<i>Plasticity</i>	
	WC-ACC	min-ACC	WF ¹⁰	WF ¹⁰⁰	WP ¹⁰	WP ¹⁰⁰
MNIST						
1	77.7 \pm 3.5	73.0 \pm 4.4	18.4 \pm 3.7	21.2 \pm 3.7	84.9 \pm 1.5	95.5 \pm 1.5
10	81.3 \pm 0.9	77.4 \pm 1.1	16.4 \pm 1.1	17.2 \pm 1.1	94.5 \pm 1.2	97.5 \pm 1.4
100	92.3 \pm 0.2	91.3 \pm 0.2	4.6 \pm 0.3	6.0 \pm 0.3	97.1 \pm 1.4	97.2 \pm 1.5
1000	92.3 \pm 0.2	91.3 \pm 0.2	4.6 \pm 0.3	6.0 \pm 0.3	97.1 \pm 1.4	97.2 \pm 1.5
CIFAR10						
1	17.9 \pm 0.9	0.0 \pm 0.0	71.1 \pm 1.8	76.0 \pm 2.0	57.7 \pm 2.3	81.4 \pm 1.1
10	18.3 \pm 0.5	0.1 \pm 0.2	71.0 \pm 3.3	74.4 \pm 1.7	78.0 \pm 3.3	89.2 \pm 0.9
100	17.4 \pm 1.8	2.0 \pm 2.5	65.9 \pm 3.1	71.4 \pm 3.2	86.9 \pm 1.8	87.1 \pm 1.6
1000	17.0 \pm 1.1	0.4 \pm 0.5	66.0 \pm 3.4	70.2 \pm 1.7	86.0 \pm 1.9	86.1 \pm 1.9
Mini-Imagenet						
1	4.1 \pm 0.3	0.5 \pm 0.2	56.6 \pm 0.9	64.6 \pm 1.1	49.3 \pm 1.6	67.6 \pm 0.7
10	5.0 \pm 0.4	1.4 \pm 0.5	60.9 \pm 0.5	63.0 \pm 0.6	65.3 \pm 0.3	68.1 \pm 0.4
100	6.7 \pm 0.4	3.1 \pm 0.4	58.8 \pm 0.6	60.5 \pm 0.7	67.0 \pm 0.7	67.2 \pm 0.8
1000	7.1 \pm 1.1	3.6 \pm 1.1	57.7 \pm 0.5	59.3 \pm 0.3	66.1 \pm 0.8	66.3 \pm 0.9
Mini-DomainNet						
1	13.7 \pm 1.0	9.6 \pm 1.0	15.1 \pm 1.4	17.8 \pm 1.2	10.2 \pm 0.6	16.9 \pm 0.7
10	15.1 \pm 1.6	11.0 \pm 1.7	14.8 \pm 0.5	15.7 \pm 0.5	14.3 \pm 0.9	22.0 \pm 0.9
100	18.3 \pm 1.1	15.8 \pm 1.3	10.0 \pm 0.8	10.0 \pm 0.8	20.6 \pm 1.0	21.0 \pm 0.8
1000	18.9 \pm 1.8	16.5 \pm 1.9	10.0 \pm 1.2	10.0 \pm 1.2	21.0 \pm 1.6	21.0 \pm 1.6

C.3 Tractable continual evaluation: Subsampling the evaluation sets

In the main paper we discuss subsampling the evaluation sets and report results for Mini-Imagenet in Table 2. Here we report the full results in Table 5 for MNIST, CIFAR10, and Mini-Imagenet.

Instead of the uniform sampling, an alternative but more complex sampling scheme would also be possible to restrain the number of evaluation samples. For example by measuring task similarity (e.g. via task2vec [1]) and merging test data of similar tasks in fixed capacity bins. Although this would be applicable for real-world learners, in our analysis we opt for the straightforward subsampling to avoid confounding factors rooted in the task similarity procedure.

C.4 Results for EWC on Mini-DomainNet

We briefly discussed the result for EWC in Mini-DomainNet in the main paper. Here we report the full results in Table 6, and Figure 6 illustrates the average accuracy curves of the 4 domains, indicating that EWC and finetuning perform on par for the best EWC configuration ($\lambda = 1$).

Figure 6: EWC and finetuning accuracy curves for the four tasks of Mini-DomainNet, reported as mean (\pm SD) over 5 seeds. Horizontal lines represent min-ACC averaged over seeds.

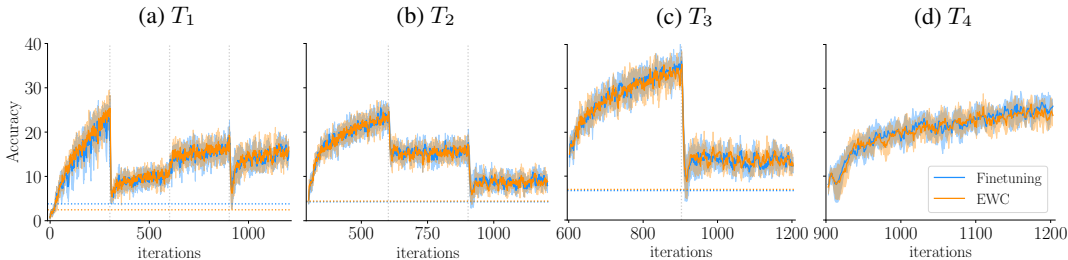


Table 5: Continual evaluation metrics for different sample sizes of the evaluation sets and comparison to training set performance on 3 benchmarks with $\rho_{eval} = 1$. 'All' indicates the full task test sets. Results over 5 seeds reported as mean (\pm SD). The Mini-Imagenet subset of the full results is reported in the main paper in Table 2. The 1000 in bold indicates the setting we applied for the other experiments in this work.

		Trade-off		Stability		Plasticity	
	Sample size	WC-ACC	min-ACC	WF ¹⁰	WF ¹⁰⁰	WP ¹⁰	WP ¹⁰⁰
MNIST							
Eval	1000	77.7 ± 3.5	73.0 ± 4.4	18.4 ± 3.7	21.2 ± 3.7	84.9 ± 1.5	95.5 ± 1.5
	100	75.1 ± 2.8	69.4 ± 3.6	25.0 ± 3.4	27.8 ± 3.3	86.9 ± 1.6	98.0 ± 1.2
	All	77.2 ± 1.4	72.3 ± 1.8	18.2 ± 1.6	20.8 ± 1.3	85.3 ± 1.3	95.0 ± 1.4
Train	1000	77.6 ± 3.5	72.6 ± 4.5	19.2 ± 4.0	22.0 ± 3.8	85.2 ± 1.8	95.7 ± 1.4
CIFAR10							
Eval	1000	17.8 ± 0.6	0.0 ± 0.0	71.3 ± 4.2	75.7 ± 2.6	59.2 ± 2.7	82.0 ± 3.3
	100	18.3 ± 0.6	0.0 ± 0.0	73.9 ± 4.3	81.7 ± 2.3	59.4 ± 2.5	86.8 ± 1.7
	All	18.1 ± 0.3	0.0 ± 0.0	73.0 ± 5.4	77.8 ± 4.9	58.6 ± 3.0	81.5 ± 4.8
Train	1000	19.3 ± 0.9	0.0 ± 0.0	75.8 ± 5.3	79.8 ± 2.7	57.8 ± 2.8	81.8 ± 2.5
Mini-Imagenet							
Eval	1000	4.1 ± 0.3	0.5 ± 0.2	56.6 ± 0.9	64.6 ± 1.1	49.3 ± 1.6	67.6 ± 0.7
	100	3.9 ± 0.5	0.3 ± 0.2	60.8 ± 2.0	71.6 ± 0.7	51.5 ± 2.7	74.3 ± 0.7
	All	4.1 ± 0.3	0.5 ± 0.2	56.0 ± 0.7	64.2 ± 0.6	48.3 ± 1.8	67.8 ± 0.4
Train	1000	5.4 ± 0.2	0.5 ± 0.2	73.8 ± 0.3	79.9 ± 0.3	50.4 ± 1.9	78.0 ± 0.5

Table 6: Mini-DomainNet continual and task-oriented evaluation results for EWC and LwF compared to ER and finetuning. The min-ACC and WF^{10/100} metrics are indicators for worst-case performance and therefore stability gaps.

Method	Trade-off		Stability				Plasticity	
	ACC	WC-ACC	min-ACC	FORG	WF ¹⁰	WF ¹⁰⁰	WP ¹⁰	WP ¹⁰⁰
Finetune	15.1 \pm 1.2	10.2 \pm 1.3	4.9 \pm 1.3	13.4 \pm 1.9	16.7 \pm 1.2	19.6 \pm 1.1	10.5 \pm 0.9	16.9 \pm 1.2
EWC	15.6 \pm 1.0	9.4 \pm 1.4	4.6 \pm 1.3	14.9 \pm 1.7	17.0 \pm 1.0	20.0 \pm 0.9	9.8 \pm 0.3	16.6 \pm 0.8
LWF	16.1 \pm 1.3	12.1 \pm 0.6	7.6 \pm 0.8	14.6 \pm 1.3	14.1 \pm 0.5	17.8 \pm 0.9	10.3 \pm 1.1	15.9 \pm 0.5
ER	21.3 \pm 2.8	14.9 \pm 1.8	11.5 \pm 1.3	3.7 \pm 1.4	11.1 \pm 1.1	13.9 \pm 1.2	8.9 \pm 1.1	14.5 \pm 1.5

C.5 Additional GEM results for MNIST and CIFAR10

The main paper shows results for MNIST accuracy curves and zooms of the stability gradient norms on task transitions. In Figure 7 we provide the full $\nabla \mathcal{L}_{\text{stability}}$ norm results during the learning process. For the analysis of the stability gap, the zoom on the task transitions is most informative, whereas the full results give an overview of gradient magnitude towards convergence of the tasks. GEM and ER are reported for the best ACC, both with learning rate 0.01 (see details in Appendix above). Compared to GEM, ER exhibits larger stability gradient norms over nearly the entire learning trajectory. This indicates that towards convergence of the task, the mini-batch gradients mostly satisfy the GEM constraints with gradient angles $\leq 90^\circ$, hence resulting in projection vectors with small magnitude. Although using the gradients of the replay samples directly for ER converges to low gradient norms, there is a notable difference for the near-zero values for GEM where these gradients are used for angle-based constraints.

Additionally to the results on MNIST, Figure 8 provides the accuracy curves for the first four tasks on CIFAR10. These results are in correspondence with literature [11, 4, 3], where GEM is not effective for the more difficult class-incremental CIFAR10 benchmark. Notable is the sharp drop to near-zero accuracy on task transitions (stability gap), which subsequently peaks and then declines rapidly.

C.6 Partial loss analysis for MNIST and CIFAR10

We report the partial ER losses $\mathcal{L}_{\text{plasticity}}$ and $\mathcal{L}_{\text{stability}}$ for the current mini-batch as additional supporting evidence for our conceptual analysis of the stability gap. It is clear from Figure 9 that the magnitude of $\mathcal{L}_{\text{plasticity}}$ is significantly higher than $\mathcal{L}_{\text{stability}}$, especially on the task transitions. The rapid decrease in plasticity loss is caused by the high gradient magnitudes, resulting in greedy updates for plasticity in the first few iterations.

Figure 7: GEM and ER per-iteration L2-norms of current $\nabla \mathcal{L}_{\text{stability}}$ on MNIST. Results reported as mean (\pm SD) over 5 seeds. Vertical lines indicate the start of a new task.

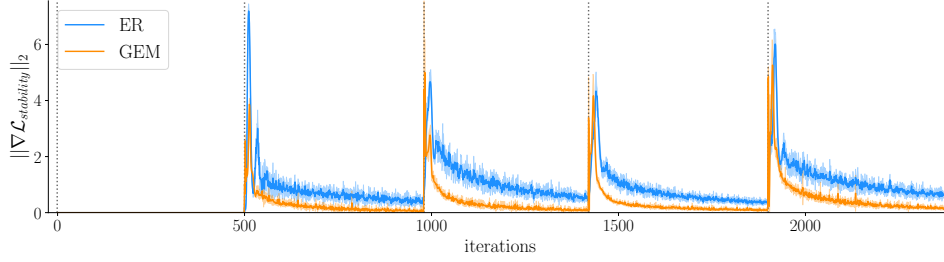


Figure 8: GEM and ER accuracy curves for the first four tasks of CIFAR10, reported as mean (\pm SD) over 5 seeds. The min-ACC averaged over seeds is zero for both methods.

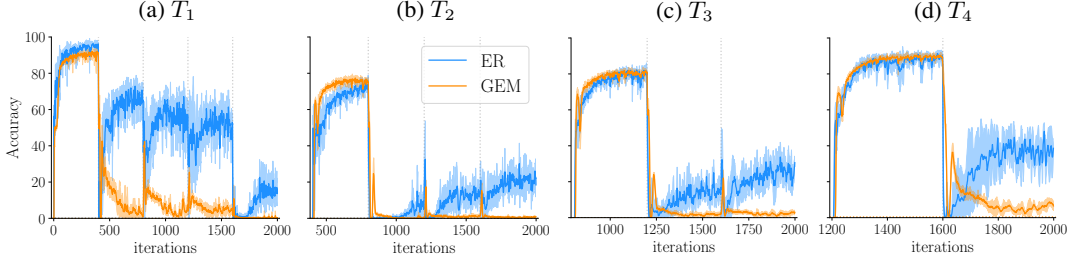


Figure 9: The partial ER losses $\mathcal{L}_{\text{plasticity}}$ and $\mathcal{L}_{\text{stability}}$ for the current mini-batch. Note the significant discrepancy of one to two orders of magnitude on the task transitions. Task transitions are indicated by the vertical lines.

